

Definition and impact of overlap on the surface state after deep rolling of aluminum and steel alloys

J. Schubnell, M. Jung, A. Sarmast and E. Carl

Fraunhofer Institute for Mechanics of Materials (IWM), Freiburg, Germany

Abstract

The mechanical surface treatment by deep rolling is a widely used process in many industrial applications to increase the fatigue and wear resistance. Multiple process parameters (contact pressure, feed rate, tool diameter) can be varied to achieve an optimum treatment result. To reduce the optimization effort for finding adequate deep rolling parameters the overlapping of two subsequent deep rolled lines was calculated assuming linear-elastic (elastic overlap factor) and elastic-plastic material behavior by analytical calculations (Hertzian contact) and by Finite Element simulation. The impact of overlapping on the surface roughness and residual stress state after deep rolling was experimentally investigated for the materials EN AW 5083, S355J2+N and S690QL. A high (elastic) overlap factor of around 90% leads to surface defects for EN AW 5083 and S355J2+N. An optimum of around 60% was determined for these materials and 90% for S690QL.

Keywords Deep rolling, Overlap factor, Residual stress, Surface roughness

Introduction

Deep rolling is a non-cutting production process which is classified as a fine surface rolling method according to VDI 3177 [1] that is used since many years in multiple industrial applications to increase the fatigue and wear resistance of crank shafts, gear wheels, spindles, screws or threads, valves, wheels rims, turbine blades etc. [2]–[4]. The fatigue life improvement by deep rolling of specimens and parts was proved for a variety of material groups in numerous investigations [4]–[8]. Hydrostatic deep rolling has the advantage that multiple parameters (contact pressure, feed rate or line spacing and tool diameter) can be separately adjusted and used for process optimization. However, experimental optimization is time-consuming and costly. Numerical simulations [9] may decrease the time effort but there are still multiple parameters that have to be considered. Due to this reasons, the aim of the present study is to introduce a easily useable so-called overlap factor that unifies the process parameters and reduces in that way the optimization effort.

Definition of overlap factor

Main parameters for deep rolling kinematics are contact pressure p , feed rate f and tool radius r_t , see Figure 1 (a). The newly introduced overlap factor O_e is defined by the overlapping area of the contact surfaces between the tool and the treated surface of two consequent passes, see Figure 1 (b). To define the contact ellipses Hertzian contact assuming elastic material behavior is utilized:

$$O_e = \frac{A_o}{A} = \frac{2}{\pi} \arccos\left(\frac{f}{2a}\right) - \frac{f}{\pi a} \sqrt{1 - \frac{f^2}{4a^2}} \quad (1)$$

$$\text{with } a = c \left(\frac{3F r}{2E^*}\right)^{\frac{1}{3}} \quad (2) \text{ and } r = 2 / \left(\frac{2}{r_t} + \frac{1}{r_w}\right) \quad (3) \text{ and } E^* = \frac{2E_t E_w}{(1 - \nu_t^2)E_w + (1 - \nu_w^2)E_t} \quad (4)$$

Where r_t is the radius of the deep rolling tool and r_w is the radius of the workpiece (for flat specimen $r_w = \infty$), E_1 and E_2 the young's modulus of deep rolling tool and workpiece and F the contact force. F can be simplified calculated by the following equation:

$$F = \pi r_t^2 p \quad (5)$$

Where p is the operating pressure of the hydrostatically supported tool. Furthermore, the constants c_1 and β were calculated according to the following equations:

$$c = \frac{2452,92}{\beta^3} + \frac{560,021}{\beta^2} + \frac{97,5878}{\beta} \quad (6) \quad \beta = \arccos\left(\frac{r}{2r_w}\right) \quad (7)$$

The overlap factor $O_e(f,p)$ depends on the process parameter f and p , as well as the materials of tool and workpiece diameter and tool diameter. In the case of a flat workpiece the stepover distance s is used instead of f . However, the plastic deformation during the process is not covered by this simplified approach. To account for elastic-plastic material behavior an alternative definition of the overlap factor O_p is introduced, that is identical with equation 1 but instead of utilizing Hertzian pressure to calculate the contact ellipse half axis a (eq. 2) the width of the contact surface is obtained by Finite Element (FE) simulation and is hereafter designated as b , see Figure 1(c) and equation 8.

$$O_p = \frac{2}{\pi} \arccos\left(\frac{f}{2b}\right) - \frac{f}{\pi b} \sqrt{1 - \frac{f^2}{4b^2}} \quad (8)$$

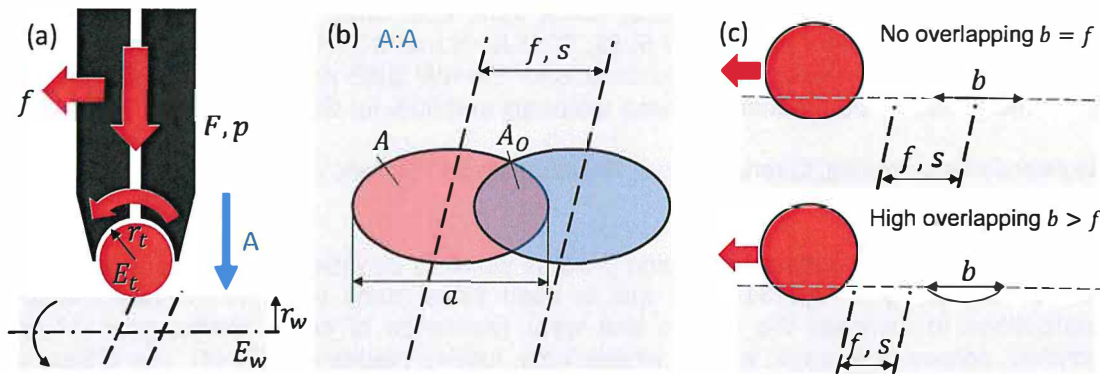


Figure 1. (a) Deep rolling process parameters, (b) overlap factor defined by contact ellipses, (c) overlap factor defined by plastic deformation of the surface after deep rolling

Material and Specimen

Three materials were investigated: The aluminum-alloy AlMg4.5Mn0.7 (EN AW 5083), the mild steel S355J2+N and the medium strength steel S690QL. The materials were chosen according to the investigations regarding deep rolling of welded joints [12,13]. The mechanical properties of this materials were determined by tensile tests according to DIN EN ISO 6892-1:2020-06 and are summarized in Table 1. The monotonic tensile curves are shown in Figure 2 (a). Deep rolling was applied with different contact pressure and feed rate at round bar specimens, shown in Figure 2 (b), at the laboratory of the Ecoroll AG. For this, a hydrostatic deep rolling tool type HG6-9 with an effective diameter of $r=6.35$ mm was used. Two rotational velocities were used, $V_u=520$ 1/min and $V_u=920$ 1/min, for S355J2+N and EN AW 5083. Altogether 33 parameter sets were investigated.

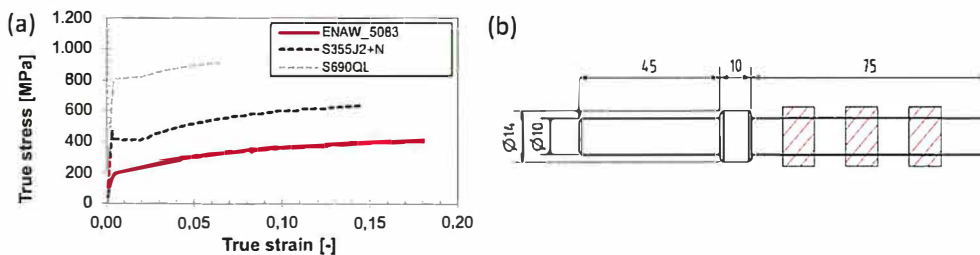


Figure 2. (a) Monotonic tensile curves of the investigated materials, (b) Specimen geometry

Table 1. Mechanical properties of the investigated materials.

	Yield strength [MPa]	Strength [MPa]	Young's modulus [GPa]	Elongation after fracture [%]	Hardness [HV10]
EN AW 5083	203	325	70	24.5	85
S355J2+N	402	505	210	32	165
S690QL	803	834	210	17	282

Determination of overlapping

The overlap factor $O_p(f, p)$ in dependence of feed rate f and contact pressure p was determined by analytical according to equation (1) to (7), as well as by FE-simulation, see Figure 3. An isotropic hardening model based on the stress-strain curves in Figure 2 (a) was used. The material behavior of the tool was assumed as linear elastic with $E=210$ GPa and $\nu=0.3$.

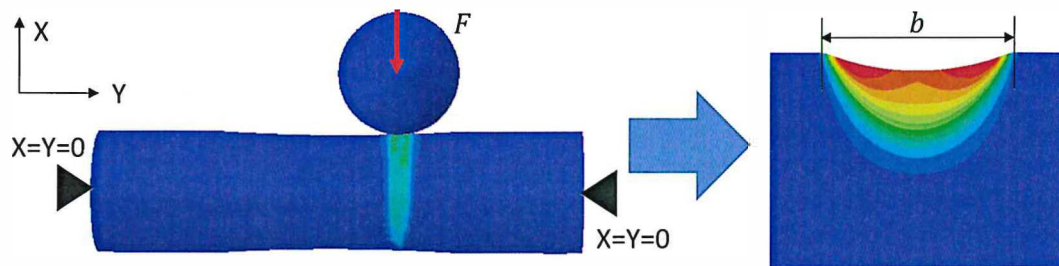


Figure 3. Finite Element model of the deep rolling process of a single line

The elastic overlap factor O_e and the plastic overlap factor O_p in dependence of the contact pressure p and the feed rate f are displayed in Figure 4. As expected, the values of O_p are significantly higher than for O_e . Also, it is shown that the overlap factors are much more influenced by feed rate than the contact pressure. High differences of O_e and O_p are determined for a feed rate $f > 0.1$ mm/rot. For lower feed rates similar values of O_e and O_p are calculated ($O_e=0.89$ and $O_p=0.97$ for $f=0.05$ mm/rot) for all materials.

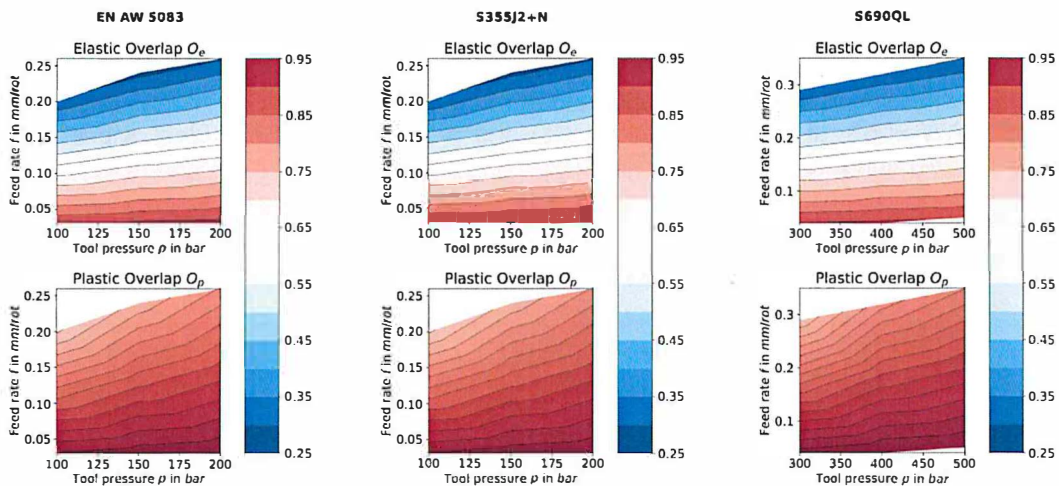


Figure 4. Influence of tool pressure and feed rate on the elastic and plastic overlap factor

Influence on the surface state

To investigate which overlap factor is needed for a proper treatment result the surface roughness and residual stress state were investigated. For all investigated parameter sets the overlap factor O_e for linear-elastic contact according to equation (1) to (7) and the overlap factor O_p based on elastic-plastic material behavior was calculated.

The surface roughness R_z and maximum roughness R_t according to DIN 4768:1990-05 was measured within 4.8 mm transverse to the rolling direction by a tactile roughness measurement device type Hommel T8000 according to DIN EN ISO 3274:1998-04. In initial condition the specimens have a roughness of $R_z=5,9 \mu\text{m}$ (EN AW 5083), $R_z=7.3 \mu\text{m}$ (S355J2+N) and $R_z=7.1 \mu\text{m}$ (S690QL). The results for R_z after deep rolling are displayed in Figure 5 in dependence of overlap factor and tool pressure. The results show that the achieved roughness is highly dependent on the tool pressure. While for EN AW 5083 and S355J2+N low pressures are favorable, S690QL shows best results with a high tool pressure. This finding points towards a dependency of the optimum tool pressure on the material's tensile strength. For all materials an elastic overlap factor of 60% and more was found to lead to the lowest surface roughness.

A high overlap factor is also not generally favorable for achieving low surface roughness. As the results for EN AW 5083 show, an overlap of 90% with a tool pressure of 150 bar leads to a very poor surface quality, see also Figure 6. Surface defects were also detected for $O_e=90\%$ for S355J2+N in combination with a high contact pressure of $p=200$ bar. In these cases, deep rolling leads to surface defects that may negatively affect the surface functions. For S690QL however, no surface defects were determined even for $O_e=90\%$ and a high contact pressure of $p=500$ bar. It is assumed that the yield strength of the material is high enough for a high intensity treatment (high overlap factor) in this case.

The surface-near residual stress state after deep rolling was determined by X-ray diffraction (XRD) analysis. The residual stresses were measured at the $\{422\}$ -aluminum lattice plane with $\text{Cu-K}\alpha$ radiation for EN AW 5083 and at the $\{211\}$ -ferritic lattice plane with $\text{Cr-K}\alpha$ radiation for S355J2+N and S690QL with a diffractometer type Bruker D8 Discover. The residual stresses in hoop- and axial-direction were measured with a collimator diameter of 1 mm. The evaluation was performed according to the $\sin^2\psi$ -method assuming a planar stress state. The constants $E=220$ GPa and $\nu=0.29$ (steel) and $E=69.7$ GPa $\nu=0.348$ (Al) were used.

The results of the XRD-analysis are summarized in Figure 7. The residual stress values were normalized with the yield strength of the materials, see Table 1. As illustrated, the residual stresses in axial direction are less affected by the variation of overlapping and contact pressure for all investigated materials. In hoop direction, a tendency is shown that a higher contact pressure for S690QL leads to higher compressive residual stresses. Furthermore, the maximum compressive residual stresses in hoop direction were measured for a lower overlapping of $O_e=30\%$ ($O_p=76\%$) for all materials. The highest compressive residual stresses in both directions were determined at $O_e=60\%$ ($O_p=76.8\%$) and $p=100$ bar for EN AW 5083, at $O_e=60\%$ ($O_p=89.3\%$) and $p=200$ bar for S355J2+N and at $O_e=90\%$ ($O_p=97.4\%$) and $p=500$ bar for S690QL.

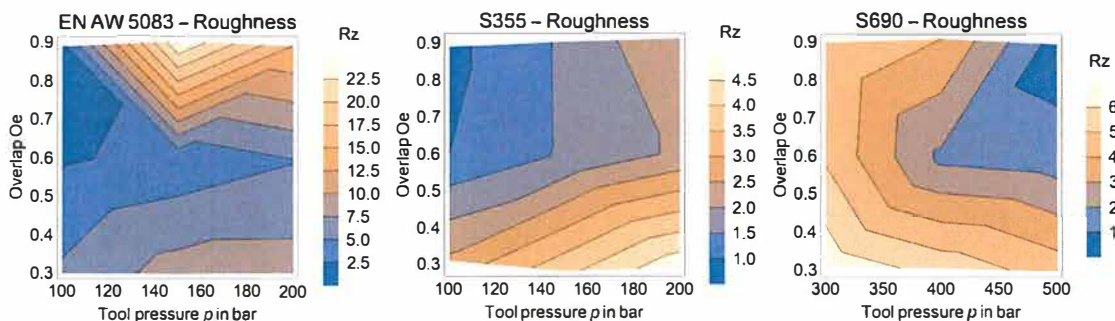


Figure 5. Impact of overlapping on the surface roughness after deep rolling

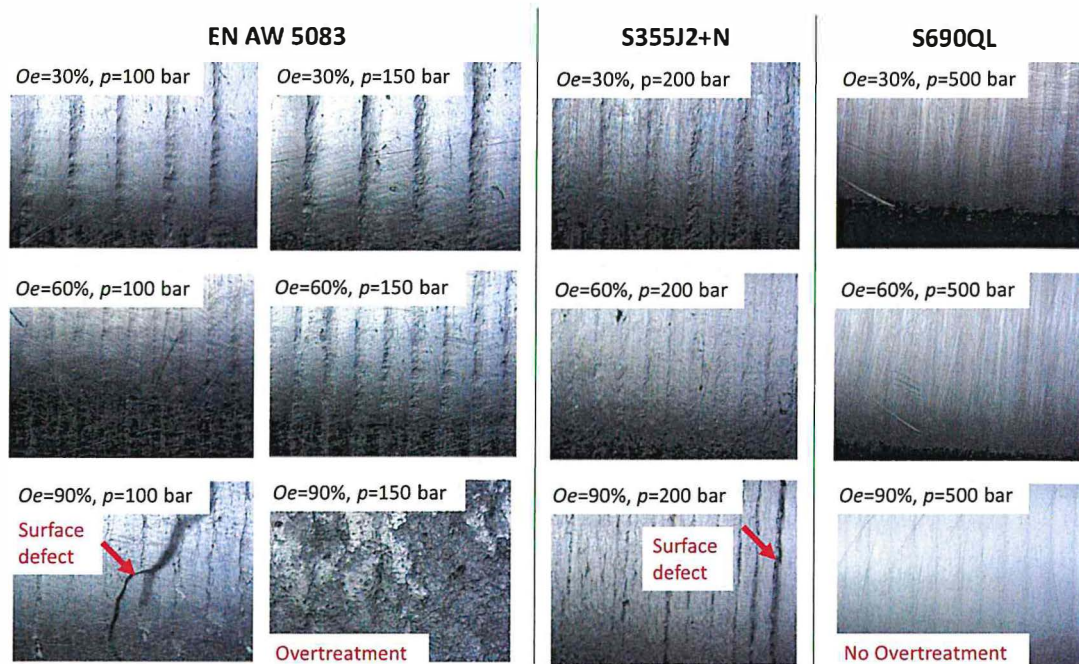


Figure 6. Impact of overlapping on the surface roughness after deep rolling

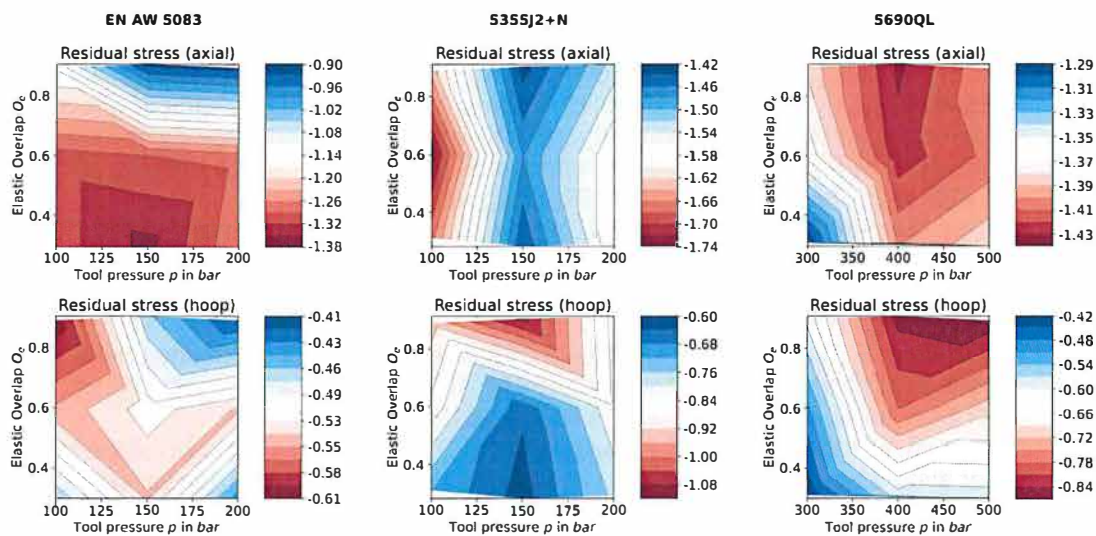


Figure 7. Impact of overlapping on the residual stress state after deep rolling

Conclusions

The overlap factor by deep rolling of subsequent treated line is defined assuming pure linear material behavior (O_e) and elastic-plastic material behavior (O_p) to reduce the optimization effort and process parameters. Round bar specimen made of EN AW 5083, S355J2+N and S690QL were deep rolled with different overlap factors. The influence of the overlap factor on surface roughness and residual stress was studied. For EN AW 5083 and S355J2+N and optimum overlap factor of $O_e=60\%$ ($O_p \approx 87\%$) with a tool pressure of 100 bar was determined. For higher values of O_e or higher tool pressure surface defects were induced by deep rolling. For S690QL a high overlap factor of $O_e=90\%$ ($O_p \approx 97\%$) does not lead to surface defects. Surface roughness was optimized by applying a high overlap factor and a high contact pressure of 500 bar. The residual stress state at the surface after deep rolling was comparably unaffected by the variation of the overlap factor. However, a high influence

of the overlap factor on the surface roughness was determined. For mild strength materials (EN AW 5083 and S355J2+N) increasing the overlap factor above the stated $O_e=60\%$ does not lead to lower surface roughness. Too high contact pressure leads to a destruction of the specimen's surface.

Funding

The IGF project „Festwalzen zur Schwingfestigkeitserhöhung bzw. Lebensdauererlängerung zyklisch beanspruchter Schweißkonstruktionen aus Stahl und Aluminiumlegierungen“ (No IGF-19537N) of the Research Association on Welding and Allied Processes of the DVS, Aachener Str. 172, 40223 Düsseldorf has been funded by the AiF within the program for sponsorship by Industrial Joint Research (IGF) of the German Federal Ministry for Economic Affairs and Climate Action based on an enactment of the German Parliament.

References

- [1] VDI, "VDI 3177:1963-03 Surface finish-rolling," 1963.
- [2] V. Schulze, *Modern Mechanical Surface Treatment: States, Stability, Effects*. New York: Wiley VCH, 2006.
- [3] V. Schulze, F. Bleicher, P. Groche, Y. B. Guo, and Y. S. Pyun, "Surface modification by machine hammer peening and burnishing," *CIRP Ann.*, vol. 65, no. 2, pp. 809–832, Jan. 2016, doi: 10.1016/J.CIRP.2016.05.005.
- [4] P. Delgado, I. I. Cuesta, J. M. Alegre, and A. Díaz, "State of the art of Deep Rolling," *Precis. Eng.*, vol. 46, pp. 1–10, Oct. 2016, doi: 10.1016/J.PRECISIONENG.2016.05.001.
- [5] G. H. Majzoobi, K. Azadikhah, and J. Nemati, "The effects of deep rolling and shot peening on fretting fatigue resistance of Aluminum-7075-T6," *Mater. Sci. Eng. A*, vol. 516, no. 1–2, pp. 235–247, Aug. 2009, doi: 10.1016/J.MSEA.2009.03.020.
- [6] I. Altenberger, R. K. Nalla, Y. Sano, L. Wagner, and R. O. Ritchie, "On the effect of deep-rolling and laser-peening on the stress-controlled low- and high-cycle fatigue behavior of Ti-6Al-4V at elevated temperatures up to 550 °C," *Int. J. Fatigue*, vol. 44, pp. 292–302, Nov. 2012, doi: 10.1016/j.ijfatigue.2012.03.008.
- [7] N. Ben Moussa, K. Gharbi, I. Chaieb, and N. Ben Fredj, "Improvement of AISI 304 austenitic stainless steel low-cycle fatigue life by initial and intermittent deep rolling," *Int. J. Adv. Manuf. Technol.* 2018 1011, vol. 101, no. 1, pp. 435–449, Nov. 2018, doi: 10.1007/S00170-018-2955-0.
- [8] S. Saalfeld, B. Scholtes, and T. Niendorf, "On the influence of overloads on the fatigue performance of deep rolled steel SAE 1045," *Int. J. Fatigue*, vol. 126, pp. 221–230, Sep. 2019, doi: 10.1016/J.IJFATIGUE.2019.05.001.
- [9] D. Trauth, F. Klocke, P. Mattfeld, and A. Klink, "Time-efficient prediction of the surface layer state after deep rolling using similarity mechanics approach," in *Procedia CIRP*, Jan. 2013, vol. 9, pp. 29–34, doi: 10.1016/j.procir.2013.06.163.
- [10] J. Schubnell, L. Mayer, E. Carl, and M. Farajian, "Deep rolling as an effective tool for the fatigue improvement of tubular welded joints," *IIV-doc. XIII-2858-2020*, 2020.
- [11] J. Schubnell and M. Farajian, "Fatigue improvement of aluminium welds by means of deep rolling and diamond burnishing," *Weld. World*, vol. 1, pp. 1–10, Dec. 2021, doi: 10.1007/S40194-021-01212-1/TABLES/5.